Electronic Supplementary Material (ESI) for Journal of Materials Chemistry C.
This journal is © The Royal Society of Chemistry 2021

Electronic Supplementary Information

Intrinsic and extrinsic defects build a novel mechanoluminescent phosphor $Na_2MgGeO_4:Mn^{2+}$

Zhongzhong Zheng,[a] Yuxing Bai,[a] Yijie Ren,[a] Huimin Chen,[a] Li Wu,*[a] Yongfa Kong,[a] Yi Zhang *[b] and Jingjun Xu [a]

[a]Key Laboratory of Weak-Light Nonlinear Photonics, Ministry of Education, School of Physics, Nankai University, Tianjin 300071, China. E-mail: *lwu@nankai.edu.cn.

[b]College of Electronic Information and Optical Engineering and Tianjin Key Laboratory of Photo-electronic Thin Film Devices and Technology, Nankai University, Tianjin 300071, China. E-mail: *yizhang@nankai.edu.cn.

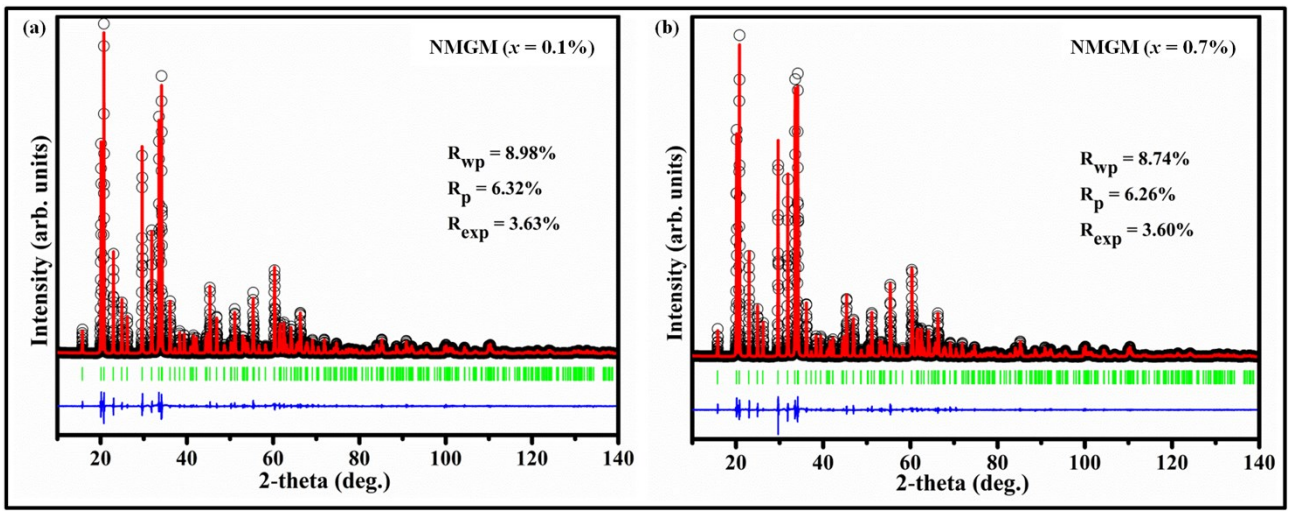

Fig. S1 The Rietveld refinement of the XRD profiles of $Na_2MgGeO_4:xMn^{2+}$ (x = 0.1% and 0.7%). Small black circles and the red continuous lines represent the experimental and the calculated values respectively; vertical bars indicate the position of Bragg peaks. The blue bottom trace depicts the corresponding residuals between the experimental and the calculated intensity values.

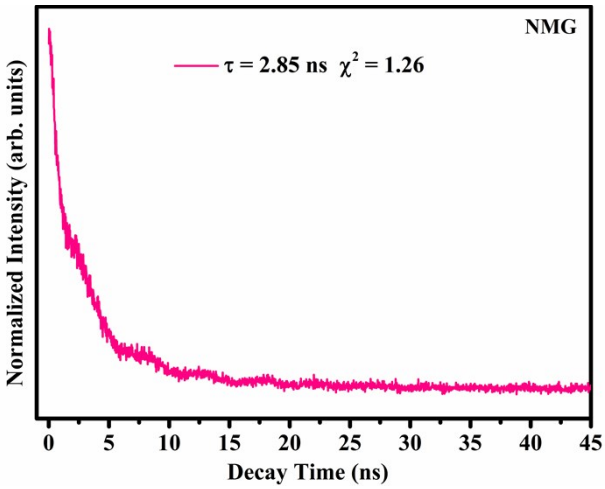

Fig. S2 Decay curves of Na_2MgGeO_4 at room temperature (λ_{ex} = 272 nm and λ_{em} = 518 nm).

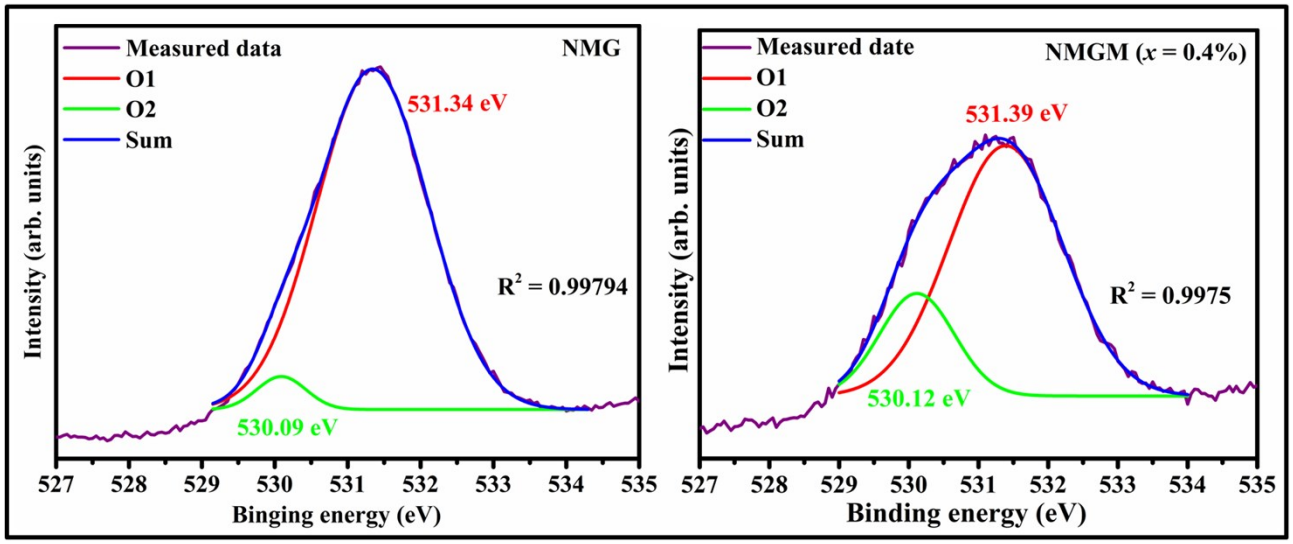

Fig. S3 The high-resolution XPS spectra of O 1*s* for Na_2MgGeO_4 and Na_2MgGeO_4:$x$$Mn^{2+}$ (x = 0.4%).

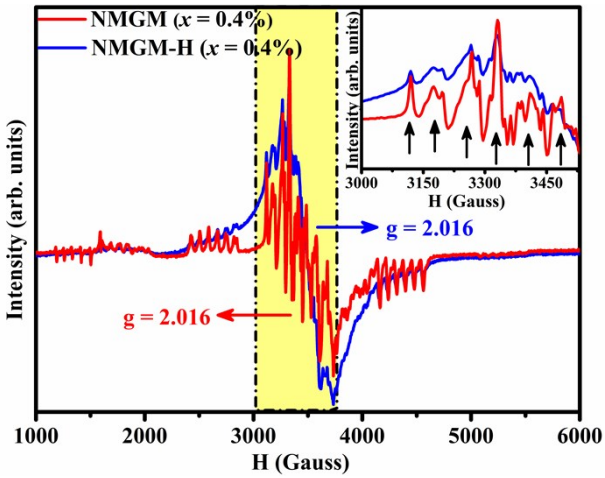

Fig. S4 The X-band powered EPR spectra of Mn^{2+} ions for Na_2MgGeO_4:$x$$Mn^{2+}$ (x = 0.4%) calcinated in ambient (NMGM) and reducing atmosphere (NMGM-H), respectively. The sextet hyperfine lines of Mn^{2+} ions in NMGM-H is hardly distinguished because

of the higher Mn^{2+} concentration in reducing atmosphere, since the EPR measurement is more sensitive to the trace Mn^{2+} ions.[1, 2]

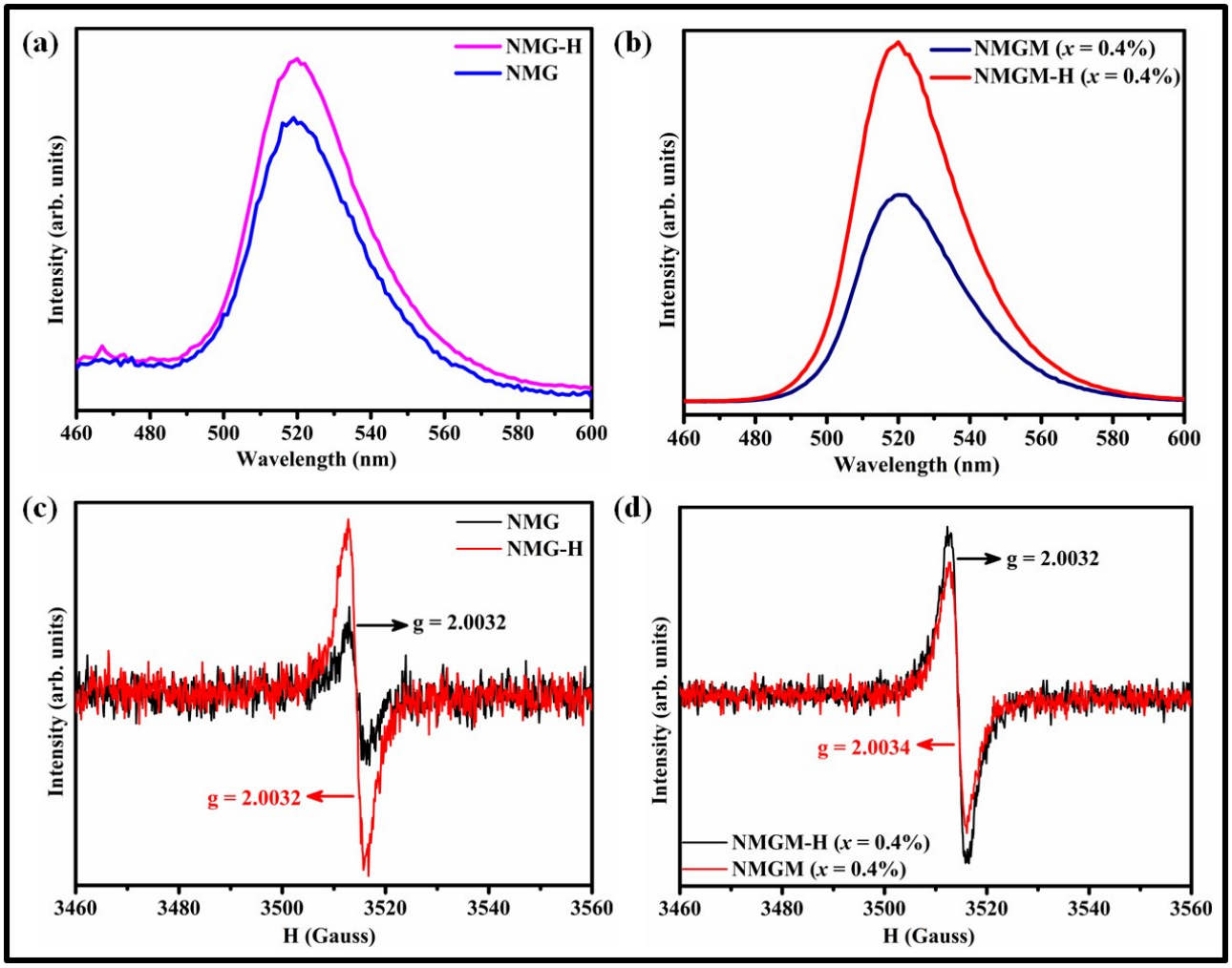

Fig. S5 (a) The PL spectra of Na_2MgGeO_4 calcinated in ambient and reducing atmosphere, respectively. (b) The PL spectra of Na_2MgGeO_4:$x$$Mn^{2+}$ (x = 0.4%) calcinated in ambient and reducing atmosphere, respectively. (c) X-band powered EPR spectra of V_O for Na_2MgGeO_4 calcinated in ambient and reducing atmosphere, respectively. (d) X-band powered EPR spectra of V_O for Na_2MgGeO_4:$x$$Mn^{2+}$ (x = 0.4%) calcinated in ambient and reducing atmosphere, respectively.

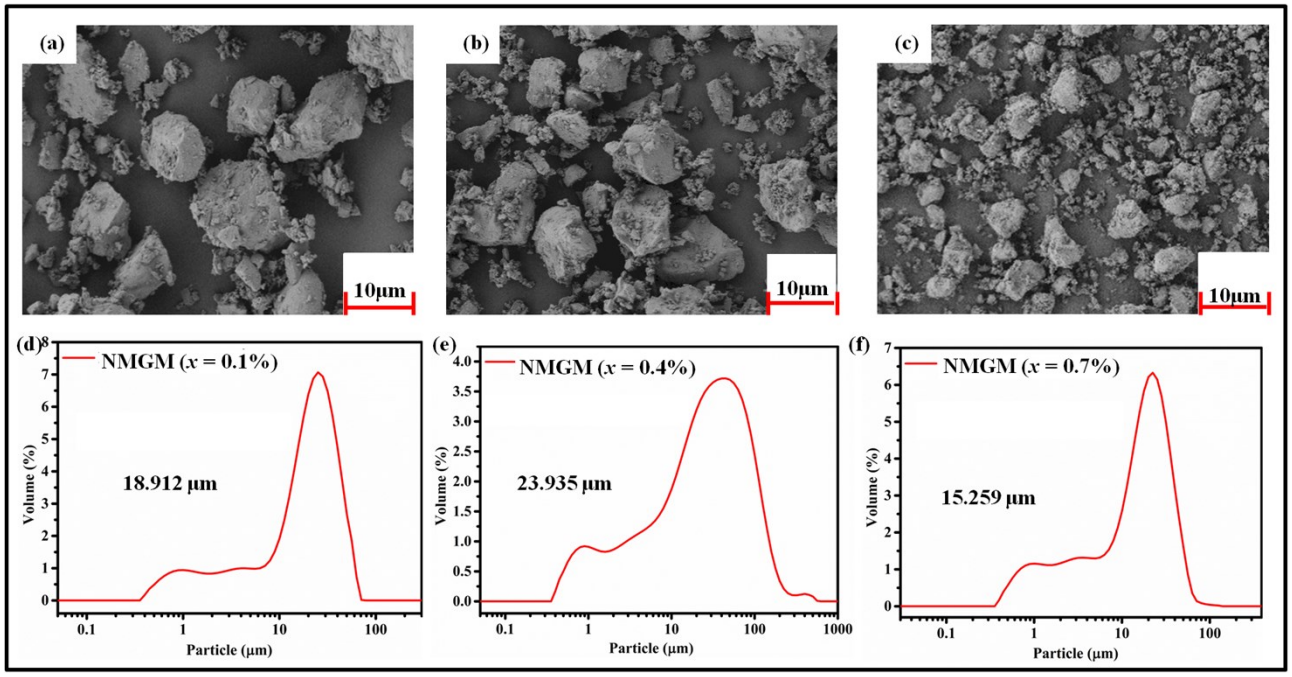

Fig. S6 (a-c) SEM images of Na_2MgGeO_4:$x$$Mn^{2+}$ (x = 0.1%, 0.4%, 0.7%). (d-f) Particle size distribution of Na_2MgGeO_4:$x$$Mn^{2+}$ (x = 0.1%, 0.4%, 0.7%). Among them, Na_2MgGeO_4:0.004Mn^{2+} has bigger average particle size, which signifies the better optical performances and coincides with the result of concentration quenching in Fig. 2e.[3]

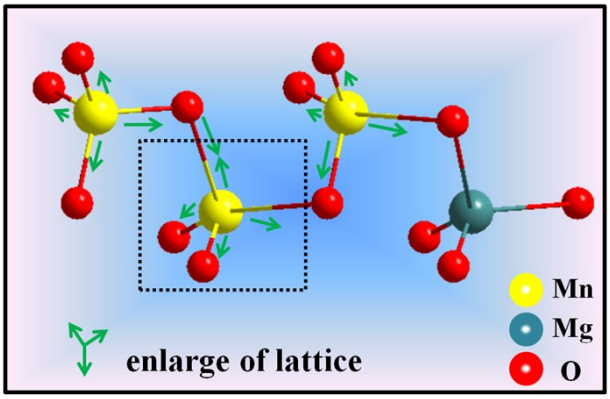

Fig. S7 Local structure coordination of Na_2MgGeO_4:Mn^{2+}. Mn^{2+} ions at selected Mg^{2+} sites are proposed for neighboring cation substitution.

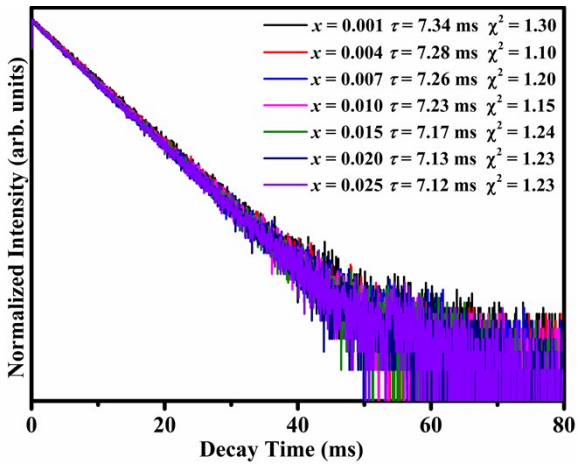

Fig. S8 Decay curves of Na_2MgGeO_4:$x$$Mn^{2+}$ ($0.001 \leq x \leq 0.025$) at room temperature (λ_{ex} = 280 nm and λ_{em} = 518 nm).

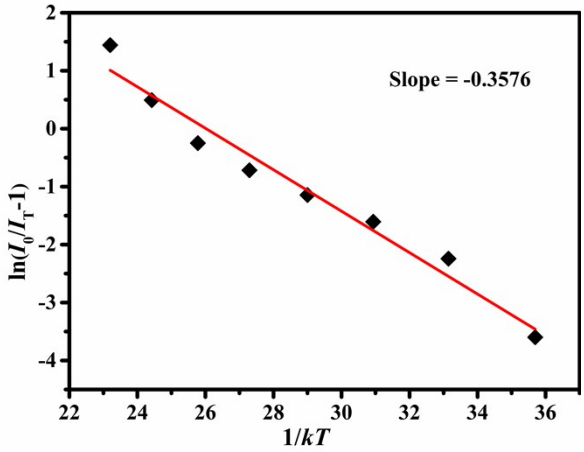

Fig. S9 The $\ln(I_0/I_T-1)$ vs. $1/kT$ activation energy graph for thermal quenching of Na_2MgGeO_4:$x$$Mn^{2+}$ (x = 0.4%).

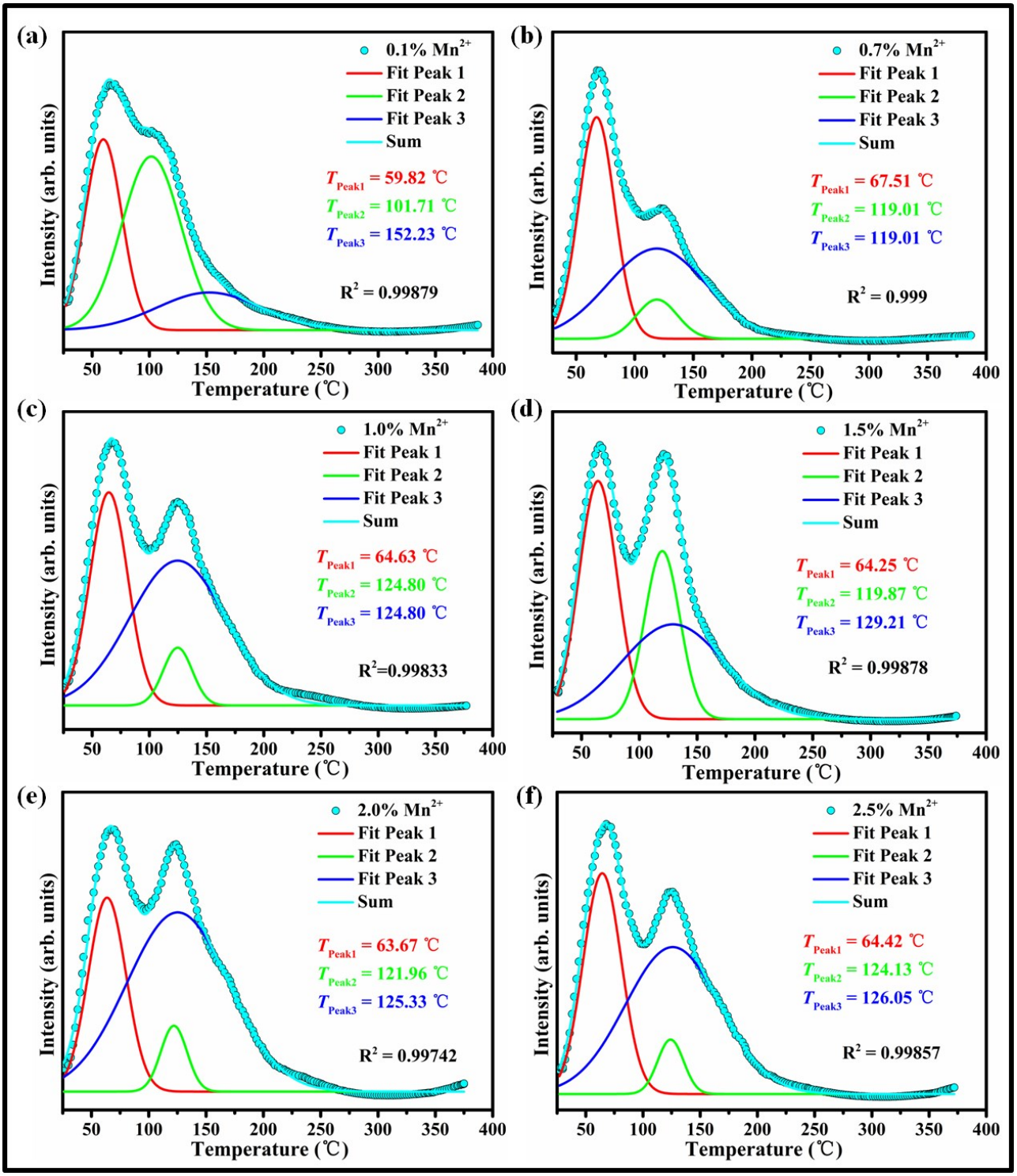

Fig. S10 Gaussian peak results of thermoluminescence curves of Na_2MgGeO_4:$x$$Mn^{2+}$ ($0 \leq x \leq 0.025$).

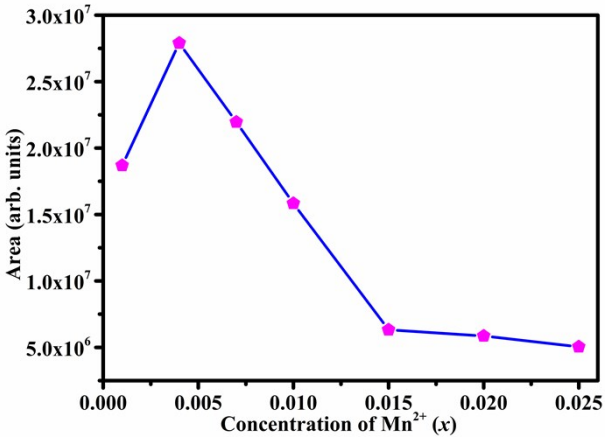

Fig. S11 The integrated area versus Mn^{2+} concentration of Na_2MgGeO_4:$x$$Mn^{2+}$ ($0 \le x \le 0.025$).

Table S1 Lattice parameters and agreement factors for Na_2MgGeO_4:$x$$Mn^{2+}$ (x = 0.4%) refined by Rietveld method, when Mn^{2+} ions occupy all kinds of the cationic sites.

Doped concentration	x = 0.004
Crystal system	monoclinic
Space group	Pc
a (Å)	5.34384(6)
b (Å)	5.61866(6)
c (Å)	8.92551(13)
β (deg)	126.8143(10)
Volume (Å^3)	214.548(5)
Z	2
R_p (%)	7.01
R_{wp} (%)	9.72
R_{exp} (%)	3.65

Table S2 Occupancy of Mn^{2+} occupying all the cationic sites for Na_2MgGeO_4:$x$$Mn^{2+}$ (x = 0.4%) refined by Rietveld method.

	site	x	y	z	Occupancy
Na1	2a	0.511(7)	0.817(2)	0.425(3)	1.043(9)
Mn1	2a	0.511(7)	0.817(2)	0.425(3)	-0.043(9)
Na2	2a	0.742(5)	0.6756(14)	0.169(3)	1.403(3)
Mn2	2a	0.742(5)	0.6756(14)	0.169(3)	-0.403(3)
Mg	2a	0.018(7)	0.185(2)	0.425(4)	0.997(9)
Mn3	2a	0.018(7)	0.185(2)	0.425(4)	0.003(9)
Ge1	2a	0.2906(4)	0.3147(5)	0.1943(3)	0.9995(8)
Mn4	2a	0.2906(4)	0.3147(5)	0.1943(3)	0.0005(8)
O1	2a	0	0.149(3)	0	1.0
O2	2a	0.165(6)	0.623(3)	0.162(3)	1.0
O3	2a	0.350(7)	0.217(3)	0.400(3)	1.0
O4	2a	0.576(6)	0.274(3)	0.157(4)	1.0

Table S3 Lattice parameters and agreement factors for Na_2MgGeO_4:0.001Mn^{2+}, Na_2MgGeO_4:0.004Mn^{2+} and Na_2MgGeO_4:0.007Mn^{2+} refined by Rietveld method.

Doped concentration	x = 0.001	x = 0.004	x = 0.007
Crystal system	monoclinic	monoclinic	monoclinic
Space group	Pc	Pc	Pc
a (Å)	5.34585(10)	5.34632(8)	5.34572(12)
b (Å)	5.61991(10)	5.62016(7)	5.61944(11)
c (Å)	8.9234(2)	8.9237(2)	8.9240(3)
β (deg)	126.7590(12)	126.7603(16)	126.7641(16)
Volume (Å^3)	214.781(8)	214.813(9)	214.757(10)
Z	2	2	2
R_p (%)	6.32	6.23	6.26
R_{wp} (%)	8.98	8.92	8.74
R_{exp} (%)	3.63	3.65	3.60

Table S4 Refinement atomic positions for Na_2MgGeO_4:0.001Mn^{2+}, Na_2MgGeO_4:0.004Mn^{2+} and Na_2MgGeO_4:0.007Mn^{2+}.

	site	x	y	z	U_{eq}	Occupancy
Na_2MgGeO_4:0.001Mn^{2+}						
Na1	2a	0.482(5)	0.817(2)	0.416(3)	0.1(2)	1.0(4)
Na2	2a	0.743(6)	0.6714(12)	0.169(4)	0.1(2)	1.0(4)
Mg1	2a	0.018(7)	0.185(2)	0.425(4)	0.2(3)	0.998(4)
Mn1	2a	0.018(7)	0.185(2)	0.425(4)	0.2(3)	0.002(4)
Ge1	2a	0.285(4)	0.3148(5)	0.186(3)	0.61(9)	1.0(4)
O1	2a	0	0.150(3)	0	0.6(2)	0.9(3)
O2	2a	0.173(6)	0.617(2)	0.170(5)	0.6(2)	0.9(3)
O3	2a	0.363(6)	0.219(3)	0.408(3)	0.6(2)	1.0(4)
O4	2a	0.631(5)	0.280(3)	0.207(4)	0.6(2)	0.9(3)
Na_2MgGeO_4:0.004Mn^{2+}						
Na1	2a	0.474(6)	0.811(3)	0.415(4)	0.003	1.0(3)
Na2	2a	0.741(7)	0.6752(14)	0.169(4)	0.003	1.0(3)
Mg1	2a	0.018(7)	0.184(2)	0.428(4)	0.008	0.995(7)
Mn1	2a	0.018(7)	0.184(2)	0.428(4)	0.008	0.005(7)
Ge1	2a	0.279(5)	0.3141(6)	0.187(3)	0.60(9)	1.0(3)
O1	2a	0	0.153(4)	0	0.2(3)	0.9(3)
O2	2a	0.155(7)	0.620(3)	0.157(4)	0.2(3)	0.9(3)
O3	2a	0.351(6)	0.211(4)	0.403(3)	0.2(3)	0.9(3)
O4	2a	0.636(6)	0.282(3)	0.215(5)	0.2(3)	0.9(3)
Na_2MgGeO_4:0.007Mn^{2+}						
Na1	2a	0.502(7)	0.823(3)	0.425(4)	0.8(2)	1.0(7)
Na2	2a	0.760(9)	0.6738(15)	0.180(4)	0.8(2)	1.0(7)
Mg1	2a	0.035(6)	0.190(2)	0.433(4)	0.5(3)	0.994(8)
Mn1	2a	0.035(6)	0.190(2)	0.433(4)	0.5(3)	0.006(8)
Ge1	2a	0.285(5)	0.3142(5)	0.199(3)	0.95(11)	1.0(7)

O1	2a	0	0.153(4)	0	0.8(3)	1.0(7)
O2	2a	0.203(8)	0.635(3)	0.213(7)	0.8(3)	0.9(7)
O3	2a	0.361(6)	0.231(4)	0.422(3)	0.8(3)	1.0(7)
O4	2a	0.638(6)	0.283(4)	0.221(5)	0.8(3)	0.9(6)

Table S5 The amounts of all the elements for the matrix through ICP-OES analysis.

element	Na	Mg	Ge	O	Mn
wt. %	13.6651	9.7309	31.7675	44.4365	no detectable

Table S6 Fitting results of Gaussian peaks of thermoluminescence curves of all the doped samples.

Mn^{2+} (mol. %)	Peak position (°C)			R^2
	T_{Peak1}	T_{Peak2}	T_{Peak3}	
0.1	59.82	101.71	152.23	0.99879
0.4	67.22	113.07	126.03	0.99907
0.7	67.51	119.01	119.01	0.999
1.0	64.63	124.80	124.80	0.99833
1.5	64.25	119.87	129.21	0.99878
2.0	63.67	121.96	125.33	0.99742
2.5	64.42	124.13	126.05	0.99857

Supplementary Movie S1. Intense stress-ML from Na_2MgGeO_4:0.004Mn^{2+}.

References

1 V. Singh, V. Natarajan, J. J. Zhu, *Opt*. *Mater*., 2007, **30**, 468-472.

2 M. Y. Peng, X. W. Yin, P. A. Tanner, M. G. Brik, P. F. Li, *Chem*. *Mater*., 2015, **27**, 2938-2945.

3 W. N. Wang, W. Widiyastuti, O. Takashi, I. W. Lenggoro and K. Okuyama, *Chem*. *Mater*., 2007, **19**, 1723-1730.